IEEE/ASME TRANSACTIONS ON

MECHATRONICS

A JOINT PUBLICATION OF THE IEEE INDUSTRIAL ELECTRONICS SOCIETY, THE IEEE ROBOTICS AND AUTOMATION SOCIETY, THE IEEE LASERS AND ELECTRO-OPTICS SOCIETY, THE ASME DYNAMIC SYSTEMS AND CONTROL DIVISION, AND THE ASME DESIGN ENGINEERING DIVISION

AUGUST 2005 VOLUME 10 NUMBER 4 IATEFW (ISSN 1083-4435)

FOCUSED SECTION ON ADVANCED MOTION CONTROL

PAPERS

SHORT PAPERS

Design and Analysis of Pneumatic Force Generators for Mobile Robotic Systems

H. Kazerooni, *Member, IEEE*

***Abstract*—Pneumatic components are rather rugged and suitable for harsh environments and therefore are an attractive alternative for mobile robots. Many robotics control algorithms require that the robot actuators be force or torque generators, so the robot controller can impose proper torque levels onto the robot joints as required by the control algorithm. While creating a torque generator using electric actuators is relatively straightforward using current feedback, there are challenges in transforming pneumatic actuators into pure force generators. This paper develops a control algorithm to convert pneumatic actuators into force generators. Because delivered work from a pneumatic actuator is product of the actuator force and the piston's displacement, the actuator force can be effectively controlled through precise measurement of the piston's displacement and robust control of the actuator's work. This paper first develops an exact model of a pneumatic system consisting of a double-acting cylinder and a servo-valve, with the goal of providing an insight into the design and control requirements for pneumatically actuated systems. Using the model, two subjects are presented in detail: 1) derivation of a control algorithm that converts a pneumatic actuator into a force generator for robotics control applications and 2) derivation of equations that can be used to design or size the power source for mobile robotic systems, where continuous source of power is unavailable.**

***Index Terms*—Control, pneumatic, robotics.**

I. Introduction

ASSUMING the actuators of a robotic system to be a force or torque generator is a foundation for many robotics control methods. Well-known robotics control algorithms, such as the computer torque method or sliding mode controllers, require that these actuators deliver well-regulated torque to the robot's joints. This concept originated from a practice in which most high performance robotic systems were designed to be powered by electric actuators. Although one can create a torque generator using current feedback from direct-drive electric motors, the compressibility of air and nonlinearities in the servo-value cause difficulties in transforming pneumatic actuators into force or torque generators. Because of these issues, the early uses of pneumatic actuators were limited to simple and non-precise positioning applications, where actuators were controlled using on-off directional valves.

In the last few years, great strides have been made towards the development of advanced control and design methods on pneumatic systems. Bobrow and Liu [2] developed effective position controllers based on the linearization around the actuator's position mid-stroke. Later, Bobrow and Jabbari, in their seminal paper [3], described using adaptive control for force actuation and trajectory tracking. Richer and Hormuzlou, in their key paper [4], developed novel techniques using sliding-mode position controllers. Ben-Dov and Salcudean developed an effective force-controlled pneumatic actuator that allows for control of the actuator force up to 16 Hz [5], employing a model that included valve dynamics and nonlinear characteristics of the compressible flow through the valve. Substantial amount of work on pneumatic systems, in particular nonlinear modeling and control, are also given in [6]–[10]. Most nonmobile robotic systems tend to use electric power (like many factory and assembly robots) because electric power is readily available, but it is our belief that pneumatic components, which are comparatively rugged and well-suited for harsh conditions, are an attractive alternative to the mobile robots described in [11].

This paper first develops an exact model of a pneumatic system consisting of a double-acting cylinder and a servo-valve, with the goal of providing insight into the design and control requirements for pneumatically actuated systems. The modeling approach uses the thermodynamic principles of energy and mass conservation, and describes two effects: unwanted dynamics from gas compressibility in the actuator and discontinuous non-linearities in the servo-valves attributed to choked flow. Using the model, we first derive a control algorithm to regulate the work delivered by a pneumatic actuator. Because output work from a pneumatic actuator is based on the multiplication of the actuator force and the piston's displacement, through precise measurement of the piston displacement and robust regulation of the actuator's output work, one can effectively convert a pneumatic actuator into a force generator for robotics control applications.

The development of the onboard power source is key to the full realization of autonomous mobile robotic systems. It is possible to carry a large tank of nitrogen (or any inert gas) or an on-board compressor for mobile robots. Nonmobile robotic systems tend to use electric power (like many factory and assembly robots) because electric power is readily available. Pneumatic components are rather rugged and suitable for harsh environments; it is our belief that pneumatic systems are an attractive alternative for mobile robots. This paper develops a methodology to design or size the power source for a given application requirement. Experiments and examples are given to verify the theories and to facilitate the application of the equations.

Manuscript received January 30, 2004; revised May 25, 2004 and December 9, 2004. Recommended by Technical Editor C. Mavroidis. This work was supported by the Office of Naval Research under Grant N000-14-98-1-0669.

The author is with the Department of Mechanical Engineering, University of California, Berkeley, Berkeley, CA 94720 USA (e-mail: kazerooni@me.berkeley.edu).

Digital Object Identifier 10.1109/TMECH.2005.852394

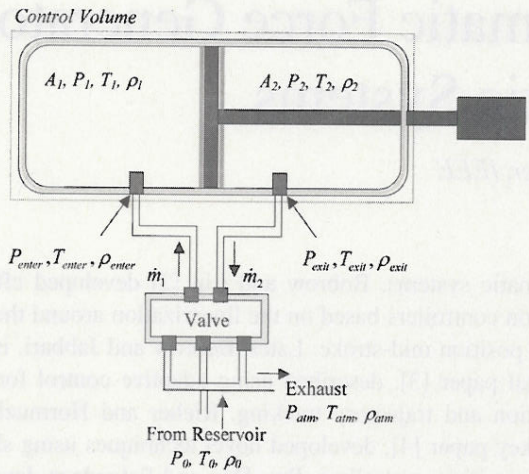

Fig. 1. Schematic of a pneumatic double acting actuator and a servo-valve.

II. Derivation of the Dynamics of a Double-Acting Actuator

The purpose of this section is to derive a set of equations representing the dynamic behavior of the pneumatic cylinder. The system consists of a double-acting linear pneumatic cylinder, fed by a 4-way servo-valve as shown in Fig. 1. Assuming that a control volume encompasses both chambers of the cylinder, and Chamber 1 is used as the intake chamber, the first law of thermodynamics can be represented by

$$\dot{Q} + \dot{m}_1\left(h_{\text{enter}} + \frac{v_{\text{enter}}^2}{2}\right) = \dot{m}_2\left(h_{\text{exit}} + \frac{v_{\text{exit}}^2}{2}\right) + \frac{\partial E}{\partial t} + \dot{W} \tag{1}$$

where

$\dot{Q}$ heat rate to the control volume;

$\dot{W}$ work rate (power) delivered by the control volume to the piston assembly;

$(\partial E/\partial t)$ rate of change of the total energy of the control volume (both chambers);

$\dot{m}_1$ mass flow rate entering the control volume;

$\dot{m}_2$ mass flow rate exiting the control volume;

h_{enter} enthalpy of the gas entering Chamber 1 (right after the servo-valve or just before going to Chamber 1);

v_{enter} velocity of the gas entering chamber 1 (right after the servo-valve or just before going to Chamber 1);

h_{exit} enthalpy of the gas exiting chamber 2 (right after Chamber 2 or just before going to servo-valve);

v_{exit} velocity of the gas exiting chamber 2 (right after Chamber 2 or just before going to servo-valve).

Below, we derive accurate equations for various elements of (1).

A. Derivation of $(\partial E/\partial t)$

The rates of change in kinetic and potential energies of the control volume are assumed to be negligible in comparison to the rate of change of the corresponding internal energy and is thus omitted. Therefore, the rate of change in the total energy of the control volume is

$$\frac{\partial E}{\partial t} = \frac{\partial (U_1)}{\partial t} + \frac{\partial (U_2)}{\partial t} \tag{2}$$

where U_1 and U_2 are the internal energies of Chambers 1 and 2, respectively, and are defined by (3) and (4), assuming ideal gas is used for the system

$$U_1 = C_V \rho_1 V_1 T_1 \tag{3}$$

$$U_2 = C_V \rho_2 V_2 T_2 \tag{4}$$

where $V_1, T_1, \rho_1, V_2, T_2$, and ρ_2 are volume, temperature, and density associated with the gas in Chambers 1 and 2, respectively. Alternatively, (3) and (4) can be written as

$$U_1 = \left(\frac{C_V}{R}\right) P_1 V_1 \tag{5}$$

$$U_2 = \left(\frac{C_V}{R}\right) P_2 V_2 \tag{6}$$

where P_1 and P_2 are the pressures in Chambers 1 and 2. C_V is the specific heat at constant volume and R is the gas constant. Substituting U_1 and U_2 from (5) and (6) into (2) results in (7) for the rate of change in energy of the control volume

$$\frac{\partial E}{\partial t} = \left(\frac{C_V}{R}\right)(\dot{P}_1 V_1 + P_1 \dot{V}_1) + \left(\frac{C_V}{R}\right)(\dot{P}_2 V_2 + P_2 \dot{V}_2). \tag{7}$$

B. Derivation of $\dot{W}$

The work rate effected on the piston assembly by the gas in the pneumatic actuator is

$$\dot{W} = P_1 \dot{V}_1 + P_2 \dot{V}_2 \tag{8}$$

where $\dot{V}_1$ and $\dot{V}_2$ are the rates of change of the volume of Chambers 1 and 2, respectively.

C. Derivation of Input and Output Enthalpies

The gas entering the actuator comes from a reservoir (usually an accumulator connected to an air compressor). Since the gas in the reservoir has zero velocity, its enthalpy is represented by the stagnation enthalpy h_o. Equation (9) describes the relationship between the stagnation enthalpy h_o and the enthalpy of the gas entering Chamber 1

$$h_{\text{enter}} + \frac{v_{\text{enter}}^2}{2} = h_o = C_P T_o \tag{9}$$

where T_o is the temperature of the gas in the accumulator. C_P, the specific heat at constant pressure, is related to the aforementioned gas constants by $C_P = C_V + R$. Similarly, the velocity of the gas in Chamber 2 is very small in comparison to the velocity of the gas exiting through the servo-valve (v_{exit}). With this assumption, (10) relates the enthalpy of Chamber 2, h_2, to the enthalpy of the gas exiting the servo-valve

$$h_{\text{exit}} + \frac{v_{\text{exit}}^2}{2} = h_2 = C_P T_2 \tag{10}$$

where T_2 is the temperature of the gas in Chamber 2. Note that the intake and exhaust enthalpies in (9) and (10) are based solely on their upstream gas temperatures.

D. Reevaluation of (1)

Substituting $\partial E/\partial t$ from (7) and the entering and existing energies from (9) and (10) into (1) results in

$$\dot{Q} + \dot{m}_1(C_P T_o) = \dot{m}_2(C_P T_2) + \left(\frac{C_V}{R}\right)(\dot{P}_1 V_1 + P_1 \dot{V}_1) + \left(\frac{C_V}{R}\right)(\dot{P}_2 V_2 + P_2 \dot{V}_2) + \dot{W}. \quad (11)$$

Further substitution of $\dot{W}$ from (8) and simplification of terms result in (12)

$$\dot{Q} + \dot{m}_1(C_P T_o) = \dot{m}_2(C_P T_2) + \left(\frac{C_V}{R}\right)(\dot{P}_1 V_1 + \dot{P}_2 V_2) + \left(1 + \frac{C_V}{R}\right)(P_1 \dot{V}_1 + P_2 \dot{V}_2). \quad (12)$$

Assuming very little heat exchange between the actuator and its surrounding, (13) represents the first law of thermodynamics for the actuator

$$\dot{m}_1(RT_0) = \dot{m}_2(RT_2) + \left(\frac{1}{k}\right)(\dot{P}_1 V_1 + \dot{P}_2 V_2) + (P_1 \dot{V}_1 + P_2 \dot{V}_2) \quad (13)$$

where $k = C_P/C_V$.

Assigning the origin ($X = 0$) to the far left end of the actuator in Fig. 1 and L as the actuator's stroke length, the chamber volumes are:

$$\begin{cases} V_1 = A_1 X \\ V_2 = A_2(L - X) \end{cases} \quad (14)$$

The derivatives of the chamber volumes are

$$\begin{cases} \dot{V}_1 = A_1 \dot{X} \\ \dot{V}_2 = -A_2 \dot{X} \end{cases} \quad (15)$$

Substituting (14) and (15) in (13) results in

$$\dot{m}_1(RT_o) - \dot{m}_2(RT_2) = \left(\frac{1}{k}\right)(\dot{P}_1 A_1 - \dot{P}_2 A_2)X + \left(\frac{1}{k}\right)\dot{P}_2 A_2 L + (P_1 A_2 - P_2 A_2)\dot{X}. \quad (16)$$

Equation (16) states how mass position X varies as one modulates the mass flow rates $\dot{m}_1$ and $\dot{m}_2$ as a function of the servo-valve opening. In other words, $\dot{m}_1$ and $\dot{m}_2$ are considered two inputs to the system and one can control them directly to alter the position of the piston rod. Derivation of $\dot{m}_1$ and $\dot{m}_2$ first requires the derivation of the dynamics of the pneumatic servo-vales, addressed below.

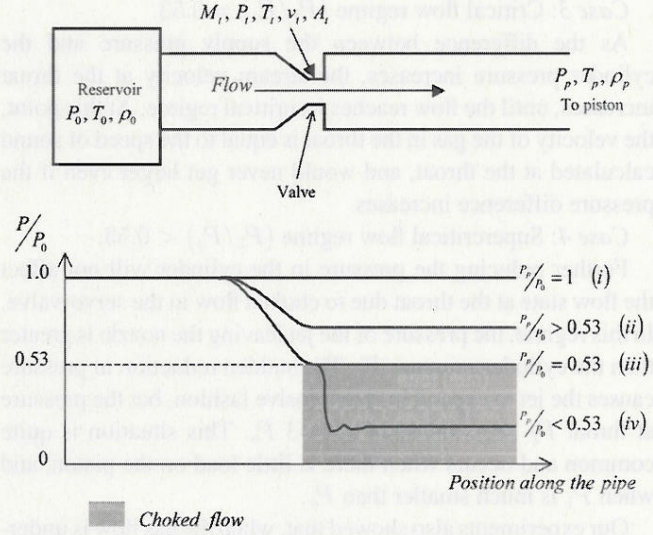

Fig. 2. Converging nozzle fed from a large reservoir is considered as a good model for the servo-valve. Other types (e.g., converging-diverging nozzels) were also investigated. However, the above converging nozzle was proven to be the most accurate model through experimental observation.

III. Derivation of the Dynamics of the Servo-Valves

The objective of this section is to calculate the mass flow rates, $\dot{m}_1$ and $\dot{m}_2$, as functions of the servo-valve opening A_T, the control variable. A converging nozzle fed from a large reservoir is considered a suitable model for the servo-valve. This converging passage discharges into Chamber 1 of the cylinder, where the pressure is P_1 (see Fig. 2). In theory, it is assumed that the gas flow in the servo-valve is adiabatic everywhere, and the flow is isentropic everywhere except across the normal shock waves. In practice, the servo-valves usually warm up and release heat to their surroundings. Therefore, the assumption of adiabatic gas flow through a converging nozzle may not be an accurate representation of the gas' behavior in the servo-valve. In order to derive a set of equations that can be used for control purposes, we need to consider this discrepancy as model uncertainty and hope that the feedback control in the system minimizes the presence of this uncertainty in the system. The possible flow patterns in the servo-valve can now be investigated based on the values of the cylinder pressure, P_1 and the supply pressure P_o

Case 1: No-flow condition: $(P_1/P_o) = 1$.

In this case, the cylinder pressure (P_1) and the supply pressure (P_o) are equal, and no flow takes place in the servo-valve from supply pressure to the cylinder. The load on the piston is so large that the piston does not move even when the servo-valve is fully open.

Case 2: Subcritical flow regime: $0.53 < (P_1/P_o) < 1$.

If the servo-valve is opened slightly, a flow with a constantly decreasing pressure will pass through the nozzle. Since the flow is subsonic at the exit plane, the throat pressure P_T must be the same as the cylinder pressure P_1. It has been shown experimentally that the pressure in the pipe from the servo-valve down to the cylinder is equal to the cylinder pressure. Thus, the pressure is uniform and equal to P_1 from near the end of the servo-valve down to the cylinder chamber.

Case 3: Critical flow regime $(P_1/P_o) = 0.53$.

As the difference between the supply pressure and the cylinder pressure increases, the stream velocity at the throat increases, until the flow reaches its critical regime. At this point, the velocity of the gas in the throat is equal to the speed of sound calculated at the throat, and would never get larger even if the pressure difference increases.

Case 4: Supercritical flow regime $(P_1/P_o) < 0.53$.

Further reducing the pressure in the cylinder will not affect the flow state at the throat due to choked flow in the servo-valve. In this regime, the pressure of the jet leaving the nozzle is greater than the cylinder pressure P_1. The sudden reduction in pressure causes the jet to expand in an explosive fashion, but the pressure at throat P_T stays constant at 0.53 P_o. This situation is quite common and occurs when there is little load on the piston, and when P_1 is much smaller than P_o.

Our experiments also showed that, when the gas flow is under-choked, the pressure at the throat and the pressure in the cylinder stay equal. When the gas flow is choked, the pressure at the throat stays at a constant 0.53 P_o, whereas the cylinder pressure decreases. The derivation of $\dot{m}_1$ and $\dot{m}_2$ as functions of the gas properties at the throat are straightforward, but the derivation of $\dot{m}_1$ and $\dot{m}_2$, as functions of the cylinder pressure, need to be developed for both choked or under-choked gas flow in the servo-valve. Note that the pressure in each chamber can be measured, but the pressure at the throat of the servo-valve cannot be measured. The values for the pressure, density, and temperature of the gas flowing through the throat of the servo-valve can be calculated from (17) to (19), regardless of the flow condition in the servo-valve

$$\frac{P_T}{P_o} = \left(1 + \frac{k-1}{2} M_T^2\right)^{\frac{k}{1-k}} \tag{17}$$

$$\frac{\rho_T}{\rho_o} = \left(1 + \frac{k-1}{2} M_T^2\right)^{\frac{1}{1-k}} \tag{18}$$

$$\frac{T_T}{T_o} = \left(1 + \frac{k-1}{2} M_T^2\right)^{-1}. \tag{19}$$

The mass flow rate at the throat of the servo-valve is defined as

$$\dot{m}_1 = \rho_T A_T v_T \tag{20}$$

where ρ_T and v_T are the density and velocity of the gas at the servo-valve throat. The velocity of the gas flow at the throat can be calculated from the definition of the Mach number M_T as follows:

$$v_T = M_T \sqrt{kRT_T}. \tag{21}$$

Substituting (17)–(19) and (21) into (20) gives the following expression for flow rate in terms of the servo-valve opening, the Mach number of the flow at the throat, and the reservoir properties:

$$\dot{m}_1 = M_T \left(1 + \frac{k-1}{2} M_T^2\right)^{\frac{k+1}{2(1-k)}} \cdot \rho_o \cdot \sqrt{kRT_o} \cdot A_T \tag{22}$$

or

$$\dot{m}_1 = M_T \left(1 + \frac{k-1}{2} M_T^2\right)^{\frac{k+1}{2(1-k)}} \cdot \sqrt{\frac{k}{RT_o}} \cdot P_o \cdot A_T. \tag{23}$$

The value of $\dot{m}_1$ depends on the exact Mach number at the throat M_T, and the servo-valve opening A_T. Inverting (17) gives the expression for the Mach number as a function of the pressure at the throat P_T

$$M_T = \sqrt{\frac{2}{k-1}} \cdot \left(\left(\frac{P_T}{P_o}\right)^{\frac{1-k}{k}} - 1\right)^{\frac{1}{2}}. \tag{24}$$

Substituting M_T from (24) into (23) results in (25), which expresses the mass flow rate as a function of the gas properties in the reservoir, the pressure at the throat, and the throat opening

$$\dot{m}_1 = \sqrt{\frac{2}{k-1}} \left(\frac{P_T}{P_o}\right)^{\frac{k+1}{2k}} \cdot \left(\left(\frac{P_T}{P_o}\right)^{\frac{1-k}{k}} - 1\right)^{\frac{1}{2}} \cdot \sqrt{\frac{k}{RT_o}} \cdot P_o \cdot A_T. \tag{25}$$

Expression (25) is valid for the gas entering the cylinder, regardless if the flow is choked or under-choked. In order to eliminate the only remaining unknown P_T, let us define γ_1 as

$$\gamma_1 = \sqrt{\frac{2}{k-1}} \cdot \left(\frac{P_T}{P_o}\right)^{\frac{k+1}{2k}} \cdot \left(\left(\frac{P_T}{P_o}\right)^{\frac{1-k}{k}} - 1\right)^{\frac{1}{2}}. \tag{26}$$

Therefore, (25) for mass flow rate can be written as

$$\dot{m}_1 = \gamma_1 \cdot \sqrt{\frac{k}{RT_o}} \cdot P_o \cdot A_T. \tag{27}$$

Now let us consider the following two cases.

Case 1: Under-choked gas flow.

When the flow is under-choked, the pressure at the throat is equal to the cylinder pressure. Therefore, γ_1 is given by (26)

$$\gamma_1 = \sqrt{\frac{2}{k-1}} \cdot \left(\frac{P_1}{P_o}\right)^{\frac{k+1}{2k}} \cdot \left(\left(\frac{P_1}{P_o}\right)^{\frac{1-k}{k}} - 1\right)^{\frac{1}{2}}. \tag{28}$$

Case 2: Choked gas flow.

When the throat is choked, the pressure at the throat stays constant. In this case, P_1 stays constant and is equal to 0.53 P_o. Substituting for P_1 into (28) results in

$$\gamma_1 = 0.58. \tag{29}$$

Therefore, the expression of the mass flow rate for gas entering the cylinder varies, depending on a choked or under-choken flow

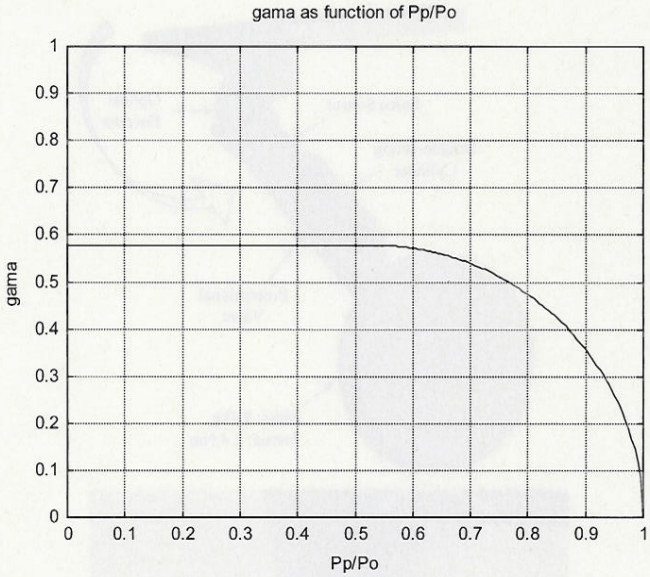

Fig. 3. γ_1 is illustrated as part of the "gain" for the mass flow rate as a function of the pressure ratio.

state. Expression (30) summarizes the above results

$$\dot{m}_1 = \gamma_1 \cdot \sqrt{\frac{k}{RT_o}} \cdot P_o \cdot A_T \tag{30}$$

if $P_1 > 0.53P_o$ (under-choked), then

$$\gamma_1 = \sqrt{\frac{2}{k-1}} \cdot \left(\frac{P_1}{P_o}\right)^{\frac{k+1}{2k}} \cdot \left(\left(\frac{P_1}{P_o}\right)^{\frac{1-k}{k}} - 1\right)^{\frac{1}{2}} \tag{31}$$

if $P_1 \leq 0.53P_o$ (choked), then

$$\gamma_1 = 0.58. \tag{32}$$

As can be seen from (30), the mass flow rate is a function of the pressure reservoir and valve opening, and Factor γ_1 can be illustrated as part of the "gain" of the throat opening in the mass flow rate expression. At low cylinder pressure values of P_1, this gain is constant ($\gamma_1 = 0.58$). As the cylinder pressure, P_1, increases, the gain decreases as shown in Fig. 3. The outgoing mass flow rate can be derived similarly, but the second chamber is now taken as a "reservoir"

$$\dot{m}_2 = \gamma_2 \cdot \sqrt{\frac{k}{RT_2}} \cdot P_2 \cdot A_T \tag{33}$$

if $P_{\text{atm}} > 0.53P_2$ (under-choked), then

$$\gamma_2 = \sqrt{\frac{2}{k-1}} \cdot \left(\frac{P_{\text{atm}}}{P_2}\right)^{\frac{k+1}{2k}} \cdot \left(\left(\frac{P_{\text{atm}}}{P_2}\right)^{\frac{1-k}{k}} - 1\right)^{\frac{1}{2}} \tag{34}$$

if $P_{\text{atm}} \leq 0.53P_2$ (choked), then

$$\gamma_2 = 0.58. \tag{35}$$

Equations (16), (30), and (33) constitute the equations for a cylinder and a servo-valve. A_T is considered an input to the system while $P_1, P_2, \dot{m}_1, \dot{m}_2$, and X are unknown. The above equations can be used on two occasions: control and design.

IV. Use of Equations for Control

The goal of this section is to derive a control algorithm that converts a pneumatic actuator to a regulated force generator. By "force generator," we mean an actuator that uses feedback to impose a precise force as a function of an input command signal. This is important for robotic control systems since most robotic control algorithms assume the robot actuators are force/torque generating systems capable of imposing exact forces/torques. To stay consistent with the conventions made previously, A_T, an algebraic area representing the area of servo-valve opening, is positive for gas entering the actuator. Most servo-valve manufacturers supply a small controller with their servo-valves so the users can accurately control the opening of the servo-valves by applying the correct voltage to the controller. Here, we assume such a servo-valve controller is available, and therefore the servo-valve opening, A_T, is proportional to a voltage command signal within a reasonably wide bandwidth. The objective is then to arrive at a practical control algorithm to convert a servo-valve and an actuator (similar to system of Fig. 1) into a force-generating system, such that the force imposed by the actuator becomes proportional to the servo-valve opening, A_T, within a bounded bandwidth. To develop such system, we start from (16). Using (30) and (33), the servo-valve equation is presented by (36)

$$\dot{m}_1(RT_o) - \dot{m}_2(RT_2) = (\gamma_1\sqrt{kRT_o}P_o - \gamma_2\sqrt{kRT_2}P_2)A_T \tag{36}$$

where γ_1 and γ_2 can be calculated from (31), (32), (34), and (35) depending on the values of (P_1/P_o) and (P_{atm}/P_2).

Assume the force the piston imposes on the mass is presented by $F_P = P_1A_1 - P_2A_2$. Equating (16) and (36) results in the following expression for (F_P), the piston force, as a function of the servo-valve opening, (A_T):

$$(\gamma_1\sqrt{kRT_o}P_o - \gamma_2\sqrt{kRT_2}P_2)A_T = \left(\frac{1}{k}\right)\dot{F}_P X + F_P\dot{X} + \left(\frac{1}{k}\right)\dot{P}_2A_2L. \tag{37}$$

Equation (37) relates the actuator force, (F_P) to (A_T), the servo-valve opening. (A_T) is considered an input while (F_P) is the output to be controlled. Since this relationship is nonlinear, the implementation of a linear controller directly on the actuator force, without further control compensation, results in inadequate force tracking for the actuator. This lack of adequate force tracking behavior (e.g., large error and low bandwidth) motivated us to investigate other possibilities for controlling the actuator force as described below.

The gas constant for air, (k), is equal to 1.4 if the gas expansion process in the actuator is adiabatic. If gas expansion process is considered isentropic (constant temperature), then $k = 1$. In a practical setting, (k) is a number between 1 and 1.4 because the gas expansion in many applications is neither adiabatic nor isentropic. For example, if a pneumatic cylinder is well

insulated and the system is designed to have a high bandwidth of operation (so gas has little time to release its energy to its surrounding), then one can comfortably assume the process is adiabatic and $k = 1.4$. On the other hand, if the system has very little insulation or if the gas expansion is slow and has ample time to exchange energy with its surrounding, then it remains at a relatively constant temperature (Isentropic) where (k) can be assumed at unity. Through our experiments, we noticed that our cylinder, like other industrial pneumatic systems, became warm and exchanged heat with its surrounding due to its slight insulation. Therefore we judged (k) to be closer to unity than 1.4, and felt rather comfortable with the assumption of $k = 1$. However, regardless of the assumption on the choice of (k), we hope that the feedback in the system (described below) minimizes the effect of this modeling uncertainty at the output.

Assuming $k = 1$, (37) can be written

$$(\gamma_1\sqrt{kRT_o}P_o - \gamma_2\sqrt{kRT_2}P_2)A_T = \frac{d}{dt}(F_P X) + \dot{P}_2 A_2 L. \tag{38}$$

Note that (X) and (F_P) are multiplied together in (38) to form an isolated variable. This prompts us to develop a controller to control and regulate $(F_P X)$ instead of (F_P). Now we choose (A_T) to equal the following equation:

$$A_T = \frac{u + \dot{P}_2 A_2 L}{(\gamma_1\sqrt{kRT_o}P_o - \gamma_2\sqrt{kRT_2}P_2)} \tag{39}$$

where (u) is a control variable. Substituting (A_T) from (39) into (38) results in (40) for the system

$$u = \frac{d}{dt}(F_P X). \tag{40}$$

Assuming $(F_P X)$ is the variable to be controlled, the system presented by (40) appears to be a first-order linear system that can be stabilized with a PD or one of many other linear controllers. In general, we choose a linear transfer function for the controller, such that

$$u(s) = K(s)(F_{\text{Desired}}X - F_P X) \tag{41}$$

to stabilize the system presented by (40), where (F_{Desired}) is the desired force. The system is only of the first order [(40)], and therefore, a proportional controller is sufficient for its stability. Note that the type of controller used is not of concern in this paper; and the most important issue is reduction of the system dynamics to a form that can be used for controller design. The term $(F_P X)$ is precisely equal to the work extracted from the piston, and (41) prescribes a controller for its regulation. At first glance, the above controller may not seem satisfactory since the work, not the force, is being regulated and therefore the accuracy of the force depends on the precision and accuracy of the piston's position (X). In other words, no matter how accurately $(F_P X)$ is controlled or regulated by $K(s)$, (F_P) may be inaccurate due to the presence of noise and/or other uncertainties in measuring (X). Although this is true in general, the piston's position (X) is a very well-measured quantity and can be measured to a very high precision with little noise. Our experiments confirmed that controlling the piston work (i.e., $F_P X$) is essentially the same as controlling the force (F_P) if a high-precision encoder is used for measuring the piston position.

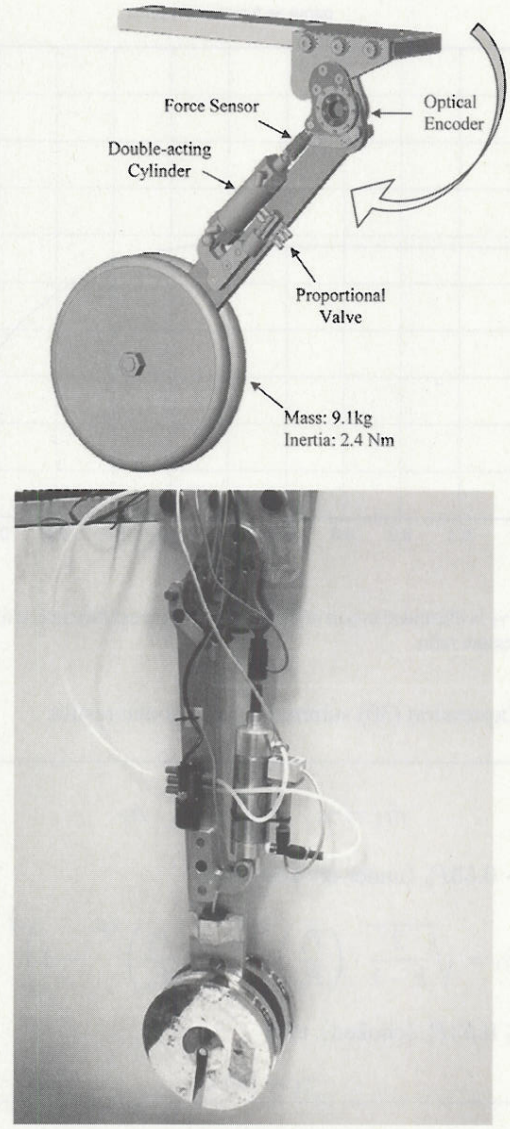

Fig. 4. Experimental system.

The experimental setup of Fig. 4 was used to verify the theories described here. A linear double-acting cylinder was used to create rotation for the mass, as shown in Fig. 4. The piston's location was calculated using precise measurement of the joint angle (4000 lines/revolution encoder) and geometrical knowledge of the system. An inline force sensor was mounted right on the piston to measure the force on the piston rod. Two pressure sensors were mounted on both sides of the piston to measure the pressure in both chambers. The measurements of these pressure sensors were used not only in (39), but also to identify the existence of the choked flow in the servo-valve. The servo-valve used was equipped with proportional flow-control and had a bandwidth of 70 Hz. As the spool was underlapped, it had no dead zone, making the system somewhat leaky but offering a wide bandwidth. A double acting actuator with a 1-in diameter was used to power the system.

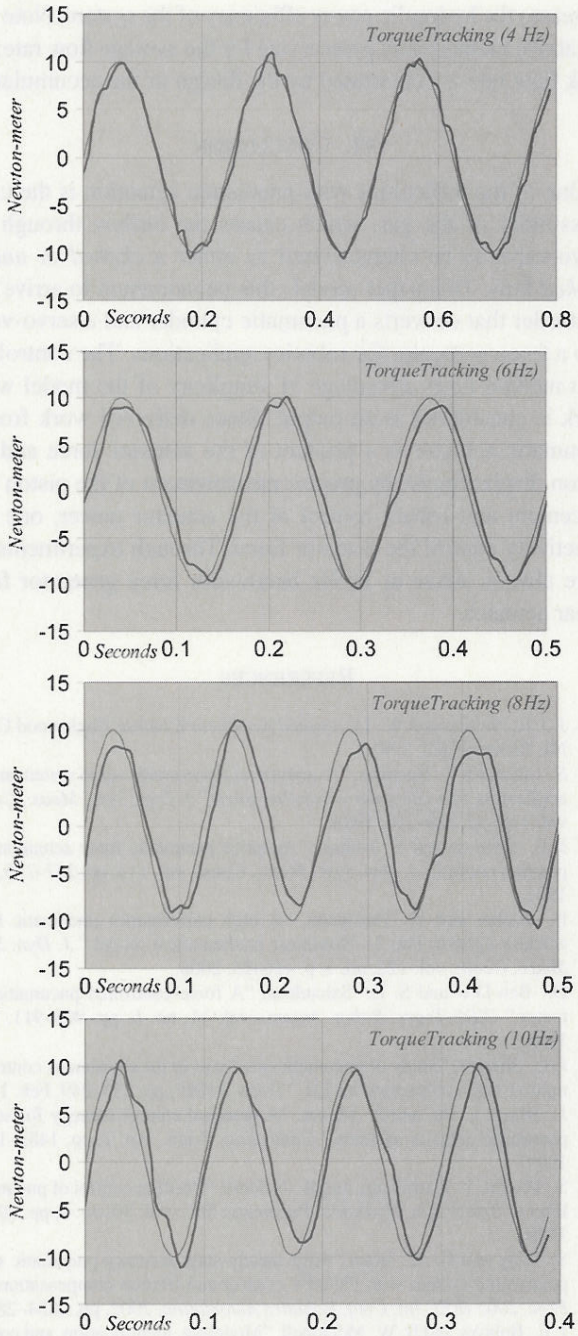

Fig. 5. Measured output torque in response to sinousoidal inputs at various frerquencies.

Fig. 5 shows the torque tracking capability of the controller when $K(s)$ was selected to be a lead-lag compensator. The experiments showed that the system was able to achieve a torque tracking capacity of up to about 10 Hz. Fig. 6 shows the ratio of the actual measured torque over the desired torque at various frequencies, where the system response attenuates at frequencies above 10 Hz. The maximum torque that can be exerted was 17 N·m. This was rather encouraging for us, since our previous attempts for torque control without the use of the model described here never allowed satisfactory tracking at frequencies above 3 Hz. We believe the improvements were due to accurate modeling of various phenomena in the servo-valve and the

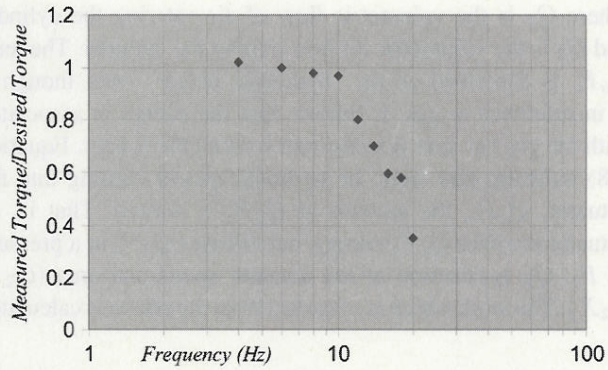

Fig. 6. System is able to track torque profiles up to 10 Hz.

cylinder. We also learned that the most important point in creating a high-bandwidth force controller is not the choice of the controller $K(s)$ but the state of the air flow in the servo-valve (i.e., choked, critically choked or under-choked). To properly assess whether the flow is choked or under-choked, and thereby choose appropriate equations for the controller, one must install precise pressure sensors on both sides of the cylinder.

V. Use of Equations for Design

This section describes results which can be used for design and component selection of a pneumatically driven robotic system. Pneumatic actuators are characterized by the area of pistons. Knowledge of the supply pressure, pressure on both sides of the cylinder, and simulation of equations described above will allow the designer to choose actuators with the appropriate piston area. One also needs to calculate the flow rate for the on-board compressor or choose the size of an onboard gas tank for a robotic application. For mobile robots the designers will need to know how much air flow is required. This question will either lead to the size of the air compressor or the size of the air tank. Compressors are sized by their flow rate at a particular pressure while compressed tanks are sized by their volume at a particular pressure (e.g., 10 gal at 1200 psi). From flow rate, designers can determine how long the robot will be able to function before refueling. The following section will evaluate how much air flow is needed to deliver an average power of $\dot{W}_{\text{Average}}$ at a given supply pressure. The derivation below allows designers to calculate the required flow rate for an on-board compressor or to choose the size of an on-board gas tank.

Equation (13) at steady state, where $\dot{P}_1 = \dot{P}_2 = 0$, can be written as

$$\dot{m}_1(RT_o) = \dot{m}_2(RT_2) + \dot{W}_{\text{Average}}. \tag{42}$$

The mass flow rate is constant

$$\dot{m}_2 = \rho_2 Q_2 = \rho_o Q_o = \dot{m}_2 = \rho_2 Q_2 \tag{43}$$

where Q_o, Q_1, and Q_2 are volumetric air flows. Substituting for $\dot{m}_1$ and $\dot{m}_2$ from (43) into (42) results in the following equation for volumetric flow rate Q_o:

$$\rho_o Q_o(RT_o) = \rho_2 Q_2(RT_2) + \dot{W}_{\text{Average}} \tag{44}$$

$$P_o Q_o = P_2 Q_2 + \dot{W}_{\text{Average}} \tag{45}$$

where Q_o is the volumetric flow of air entering the cylinder and Q_2 is the volumetric air flow exiting the cylinder. The term Q_oP_o is described as the "hydraulic power" even though it is in reference to gas. It follows that the energy is associated with the gas but does not consider its sensible energy. Equation (38) indicates that from the hydraulic power coming into the actuator, Q_oP_o, the amount of Q_2P_2 is wasted. That is, an actuator receives Q_oP_o energy, but releases Q_2P_2 at a pressure of P_2. Q_2 is function of the actuator speed and area ($Q_2 = A_2\dot{X}$). The work which is extracted from the piston is calculated as

$$\dot{W}_{\text{Average}} = \dot{X}F_{\text{Piston}} \tag{46}$$

or

$$\dot{W}_{\text{Average}} = \dot{X}(P_oA_1 - P_2A_2). \tag{47}$$

Substituting for $\dot{X}$ results in

$$\dot{W}_{\text{Average}} = \frac{Q_2}{A_2}(P_oA_1 - P_2A_2). \tag{48}$$

Substituting for Q_2 from (48) into (45) results in

$$Q_o = \frac{\dot{W}_{\text{Average}}}{\left(P_o - P_2\frac{A_2}{A_1}\right)}. \tag{49}$$

Equation (49) prescribes the required flow from a reservoir (a compressor or a tank) at the pressure of P_o. Equation (49) agrees well with our observation that for a given amount of required power, more flow is needed if gas is released from the actuator at a higher pressure.

A. Design Example

In an application, one requires 1 HP average power to power 6 DOF of a robotic system. The actuators and servo-valves are limited to function at maximum pressure of 250 psi (1.723 MP) based on manufacturer specifications. How much gas flow (or what size gas tank) is needed to extract 1 HP work from a supply pressure of 250 psi? Considering (49), one needs to have a good guess for P_2 to calculate this figure. A good dynamic simulation of the application with a proper controller usually leads to a reasonably accurate estimate for P_2. Large values of P_2 indicate greater losses while small values for P_2 suggest more efficient systems. In fact, (49) shows that if the exhaust has little pressure ($P_2 \approx 0$), all the energy from the power supply can be used to generate work. P_2, which is an application-specific quantity, generally changes from zero to the maximum value of P_o, but this is a quantity that the designer should know from the application. Assuming for this example an average value of P_2 to be about half of P_o, and equal piston areas, the required flow rate from the compressor to produce 1 HP is

$$Q_o = \frac{(1\text{ Hp})\left(550\frac{\text{lb}\cdot\text{ft}}{\text{sec}\cdot\text{Hp}}\cdot 12\frac{\text{in}}{\text{ft}}\right)}{\left(1-\frac{A_2}{2A_1}\right)250\text{ psig}} = 52.8\text{ in}^3/\text{s}. \tag{50}$$

This is the equivalent of 0.865 l/s. Evaluating the hydraulic power of the above example implies that 1 HP energy is lost due to backpressure in the cylinder. Minimizing these losses increases the hydraulic power efficiency of the system. Note that the above method only gives a size for the average flow rate; the peak flow rate is determined by the design of the accumulator.

VI. Conclusion

One of the difficulties with pneumatic actuation is the compressibility of the gas, which causes the airflow through the servo-valve to be characterized as either a *choked* or *under-choked* flow. This paper models this phenomenon to arrive at a controller that converts a pneumatic cylinder and a servo-valve into a force generator for robotics applications. The control design method takes advantage of simplicity of the model when work is considered as an output. Since delivered work from a pneumatic actuator is a product of the actuator force and the piston displacement, by precise measurement of the piston displacement and robust control of the actuator power, one can effectively control the actuator force. Through experiments we were able to arrive at 10-Hz bandwidth force generator for a linear actuator.

References

[1] J. J. E. Slotine and W. Li, *Applied Nonlinear Control*. Englewood Cliffs, NJ: Prentice-Hall, 1991.

[2] S. Liu and J. E. Burrows, "A analysis of a pneumatic servo system and its application to a computer-controlled robot," *J. Dyn. Syst., Meas., Contr.*, vol. 110, pp. 228–235, 1988.

[3] J. E. Bobrow and F. Jabbari, "Adaptive pneumatic force actuation and position control," *J. Dyn. Syst., Meas., Contr.*, vol. 113, pp. 267–276, Jun. 1991.

[4] E. Richer and Y. Hurmuzlu, "A high performance pneumatic force actuator system: Part I—Nonlinear mathematical model," *J. Dyn. Syst., Meas., Contr.*, vol. 122, no. 3, p. 416425, 2000.

[5] D. Ben-Dov and S. E. Salcudean, "A force-controlled pneumatic actuator," *IEEE Trans. Robot. Autom.*, vol. 11, no. 6, pp. 906–911, Dec. 1995.

[6] J. L. Shearer, "Study of pneumatic processes in the continuous control of motion with compressed air I,II," *Trans. ASME*, pp. 233–249, Feb. 1956.

[7] J. Wang, J. Pu, and P. Moore, "A practical control strategy for servo-pneumatic actuator systems," *Contr. Eng. Pract.*, vol. 7, pp. 1483–1488, 1999.

[8] S. Maeda, Y. Kawakami, and K. Nakano, "Position control of pneumatic lifters," *Trans. Jpn. Hydraulic Pneumatic Soc.*, vol. 30, no. 4, pp. 89–95, 1999.

[9] S. Ning and G. M. Bone, "High steady-state accuracy pneumatic servo positioning system with PVA/PV control and friction compensation," in *Proc. 2002 IEEE Int. Conf. Robotics Automation*, 2002, pp. 2824–2829.

[10] J. E. Bobrow and B. W. McDonell, "Modeling, identification, and control of a pneumatically actuated, force controllable robot," *IEEE Trans. Robot. Autom.*, vol. 14, no. 5, pp. 732–742, Oct. 1998.

[11] M. Goldfarb, E. J. Barth, M. A. Gogola, and J. A. Wehrmeyer, "Development of a hot gas actuator for self-powered robots," in *Proc. 2003 IEEE Int. Conf. Robot. Autom.*, 2003, pp. 188–193.

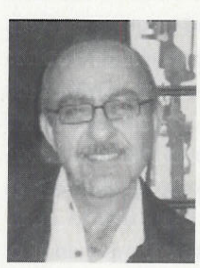

H. Kazerooni (M'84) received the M.S. and Ph.D. degrees in mechanical engineering from the Massachusetts Institute of Technology, Cambridge, in 1982 and 1984, respectively.

He is currently a Professor in the Mechanical Engineering Department and the director of the Berkeley Robotics and Human Engineering Laboratory at the University of California, Berkeley.